Differential Optical 8-PSK with Direct Detection (8-DPSK/DD)

Michael Ohm and Joachim Speidel
Institut für Nachrichtenübertragung
Universität Stuttgart, Pfaffenwaldring 47, 70569 Stuttgart, Germany
E-Mail: ohm@inue.uni-stuttgart.de

***Abstract* – We present a differential optical 8-level phase modulation scheme for direct detection with a spectral efficiency of 3 bit/symbol. The transmitter uses binary electrical signals only to produce the 8-level optical signal. The receiver consists of optical delay & add filters, O/E converters and nonlinear electrical signal processing devices. Because of proper precoding, the receiver outputs are three electrical signals, which are fed into binary decision devices for threshold detection. The spectral properties and the eye opening penalty in the presence of chromatic dispersion are analyzed for a bit rate of 60 Gbit/s and compared to intensity modulated and DQPSK signals.**

I. Introduction

The most wide spread modulation format in optical fiber transmission systems is binary intensity modulation with direct detection (IM/DD). Differential phase-shift-keying (DPSK) has also been suggested for dense wavelength-division multiplexing (DWDM) systems because of a higher robustness in the case of fiber nonlinearities [1]. In both formats, only one bit per symbol is transmitted, leading to rather poor spectral efficiencies. Recently, two quaternary optical modulation formats with DD have been proposed, which allow the transmission of 2 bits per symbol: Combined amplitude-shift-keying/phase-shift-keying with DD (ASK-PSK/DD) [2] and optical differential quaternary phase-shift-keying (DQPSK) [3].

We introduce a differential 8-PSK (8-DPSK) system with simple transmitter and receiver structures for transmitting 3 bits per symbol and thus increasing the spectral efficiency as compared to previously suggested systems.

The modulation scheme and the transmitter are explained in section II. The receiver structure is analyzed in section III. The differential encoder is presented in section IV. Section V discusses the performance of optical 8-DPSK. In the following we will consider the use of the NRZ format for all electrical signals.

II. 8-DPSK Modulation Scheme and Transmitter

The constellation diagram of 8-DPSK with its 8 signal points in the complex plane is shown in Fig. 1(a). All signal points s_k have the same magnitudes and the phase angles are $\varphi_k \in \{n\pi/4, n = 0, 1, \ldots, 7\}$.

The transmitter is presented in Fig. 1(b). Light from a continuous-wave (CW) laser $E_{cw}(t) = \sqrt{P}\exp(j\omega_0 t)$ is split by a cross coupler into an upper path $E_u(t) = \sqrt{P/2}\exp(j\omega_0 t)$ and a lower path $E_l(t) = j\sqrt{P/2}\exp(j\omega_0 t)$. P is the power of the CW laser and $\omega_0/(2\pi)$ the carrier frequency. $E_u(t)$ in the upper path is modulated in a Mach-Zehnder modulator (MZM) by the binary electrical signal $\tilde{b}(t)$. In the lower path the binary electrical signal $\tilde{a}(t)$ modulates $E_l(t)$ in a MZM. The modulated optical signals in the upper and lower paths can be written as

$$E_{u,m}(t) = \sqrt{P/2}\cdot b(t)\exp(j\omega_0 t), \quad (1)$$

$$E_{l,m}(t) = \sqrt{P/2}\cdot a(t)\exp(j\omega_0 t). \quad (2)$$

The additional phase shift of $3\pi/2$ in the lower path as seen in Fig. 1(b) is already considered in (2). The MZM are biased in such a way, that with the unipolar electrical drive signals $\tilde{b}(t)$ and $\tilde{a}(t)$ (0 for bit '0', V_π for bit '1'), $b(t)$ in (1) and $a(t)$ in (2) become -1 for bit '0' and $+1$ for bit '1'. V_π is the voltage that causes a phase difference of π in the arms of the Mach-Zehnder modulator. After combination in the following cross coupler we get the optical signal

$$E_c(t) = \frac{\sqrt{P}}{2}[b(t) + ja(t)]\exp(j\omega_0 t)$$

$$= \frac{\sqrt{P}}{2}\sqrt{b^2(t) + a^2(t)}\exp\{j[\omega_0 t + \varphi_1(t)]\}. \quad (3)$$

$E_c(t)$ is a 4-PSK signal similar to the one in [3] with

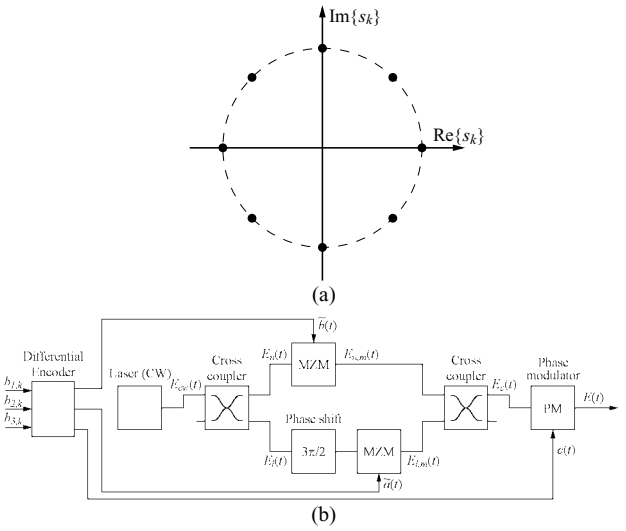

Fig. 1. 8-DPSK modulation scheme and transmitter: (a) constellation diagram and (b) transmitter structure.

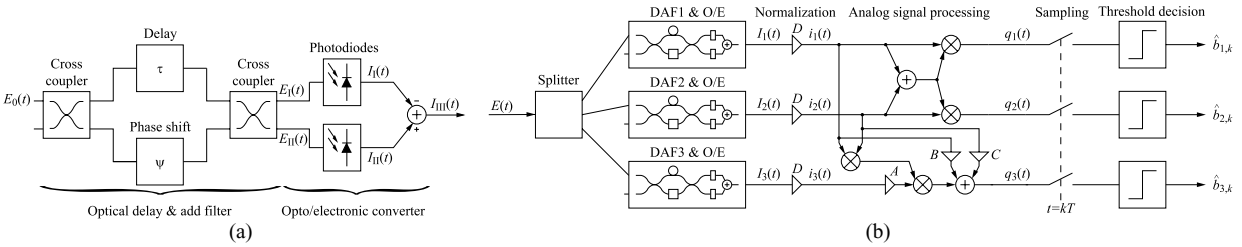

Fig. 2. (a) Optical delay & add filter. (b) 8-DPSK receiver with optical and electrical signal processing and binary decision devices

$\varphi_1(t) = arc\tan[a(t)/b(t)]$. At the time instants $t = kT$, the phase angle is $\varphi_1(kT) \in \{\pi/4, 3\pi/4, 5\pi/4, 7\pi/4\}$. T is the symbol duration.

In the following phase modulator the binary electrical signal $c(t)$ induces an additional phase shift of $\pi/4$ for bit '1' or leaves the optical signal unaltered for bit '0'. The electrical field strength of the optical signal at the output of the transmitter can thus be written as

$$E(t) = \frac{\sqrt{P}}{2}\sqrt{b^2(t)+a^2(t)}\exp\{j[\omega_0 t + \varphi_1(t) + \varphi_2(t)]\}$$
$$= \frac{\sqrt{P}}{2}\sqrt{b^2(t)+a^2(t)}\exp\{j[\omega_0 t + \varphi(t)]\} \quad (4)$$

with $\varphi_2(kT) \in \{0, \pi/4\}$, and the resulting phase angle $\varphi(t) = \varphi_1(t) + \varphi_2(t)$. At the time instants $t = kT$ it becomes $\varphi(kT) \in \{n\pi/4, n = 0, 1, \ldots, 7\}$. $E(t)$ at the output of the transmitter is the desired 8-DPSK signal. The differential modulation and encoding scheme is proposed, because it leads to a simple receiver with direct detection. The 8-DPSK differential encoder function will be given at a later point, because for deriving the function, the structure of the differential receiver has to be considered first.

Looking at (3), we see that if we had allowed multilevel electrical signals $\tilde{b}(t)$ and $\tilde{a}(t)$, we could have obtained $E_c(t)$ as an 8-level signal. Multilevel electrical signals could be generated by a mapper, that maps three input bit streams onto $\tilde{b}(t)$ and $\tilde{a}(t)$. This is the standard technique in electrical quadrature amplitude modulation (QAM) [4]. However, we choose the structure in Fig. 1(b) in order to keep the electrical signals binary.

III. 8-DPSK Receiver

A. Delay & Add Filter

Before going into details of the 8-DPSK receiver, we want to shortly review the so-called delay & add filter (DAF) given in Fig. 2(a), which plays a major role in the demodulation process also for the previously mentioned modulation schemes [1-3]. The DAF consists of a cross coupler at the input, a delay line with delay τ, a path that introduces a phase shift of ψ, and another cross coupler. After the DAF, the two optical output signals are detected with photodiodes.

If the input to the DAF is $E_0(t) = \hat{E}_0\exp\{j[\omega_0 t + \varphi(t)]\}$, with the amplitude $\hat{E}_0$ of the input signal, the two outputs become

$$E_{\mathrm{I}}(t) = \frac{1}{2}[E_0(t-\tau) - \exp(j\psi)E_0(t)]$$
$$= \frac{\hat{E}_0}{2}(\exp\{j[\omega_0(t-\tau) + \varphi(t-\tau)]\}$$
$$-\exp\{j\psi\}\exp\{j[\omega_0 t + \varphi(t)]\}) \quad (5)$$

and

$$E_{\mathrm{II}}(t) = \frac{j}{2}[E_0(t-\tau) + \exp(j\psi)E_0(t)]$$
$$= \frac{j\hat{E}_0}{2}(\exp\{j[\omega_0(t-\tau) + \varphi(t-\tau)]\}$$
$$+ \exp\{j\psi\}\exp\{j[\omega_0 t + \varphi(t)]\}). \quad (6)$$

The two optical signals according to (5) and (6) are incident on two photodiodes with responsivity R, and we get two electrical signals

$$I_{\mathrm{I}}(t) = R|E_1(t)|^2$$
$$= \frac{R\hat{E}_0^2}{2}\{1 - \cos[\varphi(t) - \varphi(t-\tau) + \psi]\} \quad (7)$$

and

$$I_{\mathrm{II}}(t) = R|E_2(t)|^2$$
$$= \frac{R\hat{E}_0^2}{2}\{1 + \cos[\varphi(t) - \varphi(t-\tau) + \psi]\}. \quad (8)$$

The delay τ is chosen to $\tau = T$ in the following, and it is assumed that $\exp(j\omega_0\tau) = 1$. Further, we write $\Delta\varphi(t) = \varphi(t) - \varphi(t-T)$. Subtraction of the electrical signals yields

$$I_3(t) = I_2(t) - I_1(t) = R\hat{E}_0^2\cos[\Delta\varphi(t) + \psi]. \quad (9)$$

From (9) we conclude that we can detect phase differences between consecutive symbols with a phase offset ψ.

B. 8-DPSK Receiver structure

The receiver structure with an optical 1:3 power splitter, three DAF with O/E, a normalization stage, and analog sig-

Table 1. Values of $q_1(kT)$, $q_2(kT)$ and $q_3(kT)$ with respect to $\Delta\varphi(kT)$

$\Delta\varphi(kT)$	$q_1(kT)$	$q_2(kT)$	$q_3(kT)$	$\hat{b}_{1,k}$	$\hat{b}_{2,k}$	$\hat{b}_{3,k}$
0	1	1	1/2	1	1	1
$\pi/4$	0	1	1/2	0	1	1
$\pi/2$	0	0	1/2	0	0	1
$3\pi/4$	1	0	1/2	1	0	1
π	1	1	-1/2	1	1	0
$5\pi/4$	0	1	-1/2	0	1	0
$3\pi/2$	0	0	-1/2	0	0	0
$7\pi/4$	1	0	-1/2	1	0	0

nal processing is shown in Fig. 2(b).

The phase shifts in the DAF are set to $\psi_1 = \pi/4$ for DAF1, $\psi_2 = 7\pi/4$ for DAF2, and $\psi_3 = 15\pi/8$ for DAF3. We assume $E(t)$ according to (4) to be the input to the receiver. Further, assuming an ideal 1:3 power splitter, the electrical output signals of the DAF & O/E modules are

$$I_1(t) = [RP/(6\sqrt{2})][\cos\Delta\varphi(t) - \sin\Delta\varphi(t)], \quad (10)$$

$$I_2(t) = [RP/(6\sqrt{2})][\cos\Delta\varphi(t) + \sin\Delta\varphi(t)], \quad (11)$$

$$I_3(t) = (RP/6)\cos(\Delta\varphi(t) + 15\pi/8). \quad (12)$$

Before analog signal processing, it is necessary to have a normalization stage. After normalization with $D = 6/(RP)$ the signals are

$$i_1(t) = (1/\sqrt{2})[\cos\Delta\varphi(t) - \sin\Delta\varphi(t)], \quad (13)$$

$$i_2(t) = (1/\sqrt{2})[\cos\Delta\varphi(t) + \sin\Delta\varphi(t)], \quad (14)$$

$$i_3(t) = \cos(\Delta\varphi(t) + 15\pi/8). \quad (15)$$

With (13) and (14) we get the output signals

$$q_1(t) = [\cos\Delta\varphi(t) - \sin\Delta\varphi(t)]\cos\Delta\varphi(t), \quad (16)$$

$$q_2(t) = [\cos\Delta\varphi(t) + \sin\Delta\varphi(t)]\cos\Delta\varphi(t), \quad (17)$$

and

$$\begin{aligned} q_3(t) = {} & \frac{A}{2}\cos[\Delta\varphi(t) + 15\pi/8] \\ & \times[\cos\Delta\varphi(t) + \sin\Delta\varphi(t)][\cos\Delta\varphi(t) - \sin\Delta\varphi(t)] \\ & + \frac{B}{\sqrt{2}}[\cos\Delta\varphi(t) - \sin\Delta\varphi(t)] \\ & + \frac{C}{\sqrt{2}}[\cos\Delta\varphi(t) + \sin\Delta\varphi(t)]. \end{aligned} \quad (18)$$

If we choose

$$\begin{aligned} A &= 2/\sqrt{\sqrt{2}+2} \\ C &= -B = 1/2 \end{aligned} \quad (19)$$

the samples $q_1(kT)$, $q_2(kT)$ and $q_3(kT)$ for all possible phase differences $\Delta\varphi(kT)$ are given in Table 1. All three values are binary and the combinations are unique, so the corresponding bit sequences $\hat{b}_{1,k}$, $\hat{b}_{2,k}$ and $\hat{b}_{3,k}$ can be derived with binary decision devices. The bit values are also given in Table 1.

Typical eye diagrams for the electrical signals $q_1(t)$, $q_2(t)$ and $q_3(t)$ are shown in Fig. 3. These diagrams represent the case of an 8-DPSK system with a symbol rate $R_s = 20\,\text{Gsymbols/s}$ (i.e. 60 Gbit/s) using an optical receiver filter (Bessel 3rd order, 3-dB bandwidth $4 \cdot R_s$). All electrical signals are assumed to be bandlimited by Bessel filters (3rd order, 3-dB bandwidth $1 \cdot R_s$).

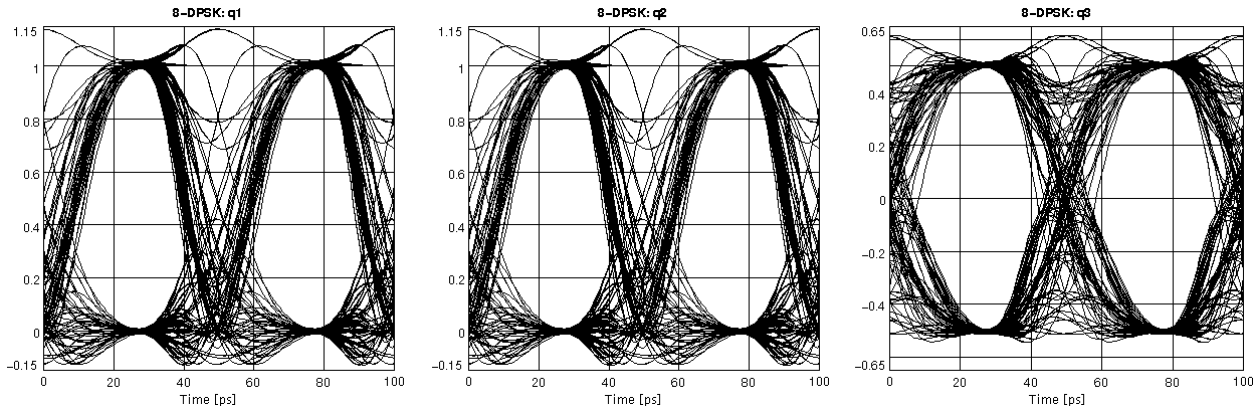

Fig. 3. Typical eye diagrams for 8-DPSK receiver output signals $q_1(t)$, $q_2(t)$, $q_3(t)$

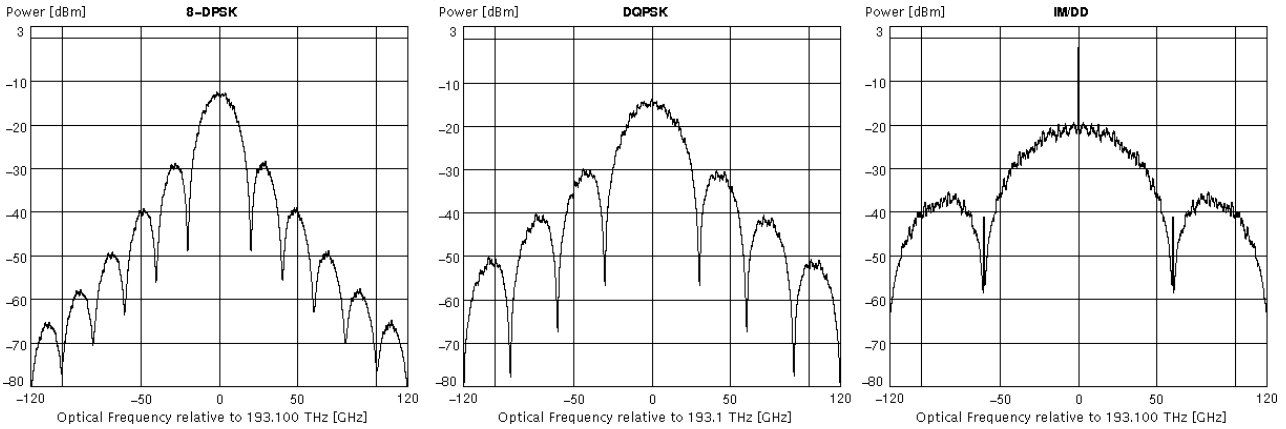

(a) (b) (c)

Fig. 4. Power spectra of (a) 8-DPSK, (b) DQPSK and (c) IM/DD with a total bit rate of 60Gbit/s

IV. Differential Encoder for 8-DPSK

With the knowledge of the receiver structure and its output signals, it is now possible to derive three differential encoding functions, so that the output bit sequences at the receiver $\hat{b}_{1,k}$, $\hat{b}_{2,k}$ and $\hat{b}_{3,k}$ are equal to the input bit streams to the differential encoder $b_{u,k}$, $b_{v,k}$ and $b_{w,k}$ in the case of error free transmission. The output bit sequences of the differential encoder are $b_{r,k}$, $b_{s,k}$ and $b_{t,k}$, which correspond to the modulator drive signals $c(t)$, $\tilde{b}(t)$ and $\tilde{a}(t)$, respectively. The functions of the differential encoder can be derived as

$$\begin{aligned} b_{r,k} = {} & \overline{b_{r,k-1}} \cdot b_{1,k} \cdot \overline{b_{2,k}} + \overline{b_{r,k-1}} \cdot \overline{b_{1,k}} \cdot b_{2,k} \\ & + b_{r,k-1} \cdot b_{1,k} \cdot b_{2,k} + b_{r,k-1} \cdot \overline{b_{1,k}} \cdot \overline{b_{2,k}}, \end{aligned} \quad (20)$$

$$\begin{aligned} b_{s,k} = {} & \overline{b_{r,k-1}} \cdot b_{s,k-1} \cdot b_{2,k} \cdot b_{3,k} \\ & + \overline{b_{r,k-1}} \cdot \overline{b_{s,k-1}} \cdot b_{2,k} \cdot \overline{b_{3,k}} \\ & + \overline{b_{r,k-1}} \cdot b_{t,k-1} \cdot \overline{b_{2,k}} \cdot \overline{b_{3,k}} \\ & + \overline{b_{r,k-1}} \cdot \overline{b_{t,k-1}} \cdot \overline{b_{2,k}} \cdot b_{3,k} \\ & + b_{s,k-1} \cdot b_{1,k} \cdot b_{2,k} \cdot b_{3,k} \\ & + \overline{b_{s,k-1}} \cdot b_{1,k} \cdot b_{2,k} \cdot \overline{b_{3,k}} \\ & + b_{s,k-1} \cdot \overline{b_{t,k-1}} \cdot \overline{b_{1,k}} \cdot b_{3,k} \\ & + \overline{b_{s,k-1}} \cdot b_{t,k-1} \cdot \overline{b_{1,k}} \cdot \overline{b_{3,k}} \\ & + \overline{b_{s,k-1}} \cdot \overline{b_{t,k-1}} \cdot \overline{b_{2,k}} \cdot b_{3,k} \\ & + b_{s,k-1} \cdot b_{t,k-1} \cdot \overline{b_{2,k}} \cdot \overline{b_{3,k}} \\ & + b_{r,k-1} \cdot b_{t,k-1} \cdot \overline{b_{1,k}} \cdot \overline{b_{3,k}} \\ & + b_{r,k-1} \cdot \overline{b_{t,k-1}} \cdot \overline{b_{1,k}} \cdot b_{3,k} \\ & + b_{r,k-1} \cdot b_{s,k-1} \cdot b_{1,k} \cdot \overline{b_{2,k}} \cdot \overline{b_{3,k}} \\ & + b_{r,k-1} \cdot \overline{b_{s,k-1}} \cdot b_{1,k} \cdot \overline{b_{2,k}} \cdot b_{3,k} \end{aligned} \quad (21)$$

and

$$\begin{aligned} b_{t,k} = {} & \overline{b_{r,k-1}} \cdot b_{s,k-1} \cdot b_{t,k-1} \cdot b_{3,k} \\ & + b_{r,k-1} \cdot b_{s,k-1} \cdot \overline{b_{1,k}} \cdot b_{3,k} \\ & + b_{r,k-1} \cdot \overline{b_{s,k-1}} \cdot \overline{b_{1,k}} \cdot \overline{b_{3,k}} \\ & + b_{t,k-1} \cdot b_{1,k} \cdot b_{2,k} \cdot b_{3,k} \\ & + \overline{b_{t,k-1}} \cdot b_{1,k} \cdot b_{2,k} \cdot \overline{b_{3,k}} \\ & + \overline{b_{r,k-1}} \cdot \overline{b_{s,k-1}} \cdot \overline{b_{2,k}} \cdot \overline{b_{3,k}} \\ & + \overline{b_{r,k-1}} \cdot \overline{b_{t,k-1}} \cdot b_{2,k} \cdot \overline{b_{3,k}} \\ & + \overline{b_{r,k-1}} \cdot b_{t,k-1} \cdot b_{2,k} \cdot b_{3,k} \\ & + \overline{b_{s,k-1}} \cdot b_{t,k-1} \cdot \overline{b_{2,k}} \cdot \overline{b_{3,k}} \\ & + b_{s,k-1} \cdot \overline{b_{t,k-1}} \cdot \overline{b_{2,k}} \cdot b_{3,k} \\ & + \overline{b_{s,k-1}} \cdot \overline{b_{t,k-1}} \cdot \overline{b_{1,k}} \cdot \overline{b_{3,k}} \\ & + b_{s,k-1} \cdot \overline{b_{1,k}} \cdot \overline{b_{2,k}} \cdot b_{3,k} \\ & + b_{r,k-1} \cdot \overline{b_{t,k-1}} \cdot b_{1,k} \cdot \overline{b_{2,k}} \cdot b_{3,k} \\ & + b_{r,k-1} \cdot b_{t,k-1} \cdot b_{1,k} \cdot \overline{b_{2,k}} \cdot \overline{b_{3,k}}. \end{aligned} \quad (22)$$

The operators '+', '·' and '¯' in (20)-(22) denote logical OR, logical AND and logical NOT, respectively. The encoding functions can be realized as look-up tables or as combinational networks.

V. Performance of 8-DPSK

We investigated the performance of 8-DPSK with computer simulations. Fig. 4(a) shows the power spectrum of an 8-DPSK signal in comparison to to the spectra of a DQPSK signal (Fig. 4(b)) according to [3] and an IM/DD signal (Fig. 4(c)). The total bit rate for all three systems is 60Gbit/s. For a given total bit rate the symbol rate of 8-DPSK is by factor 3 lower than for IM/DD and by factor 1.5 lower than for DQPSK. Thus, as can be observed in Fig. 4, the cut-off frequency of the 8-DPSK spectrum is significantly lower than those for DQPSK and IM/DD spectra.

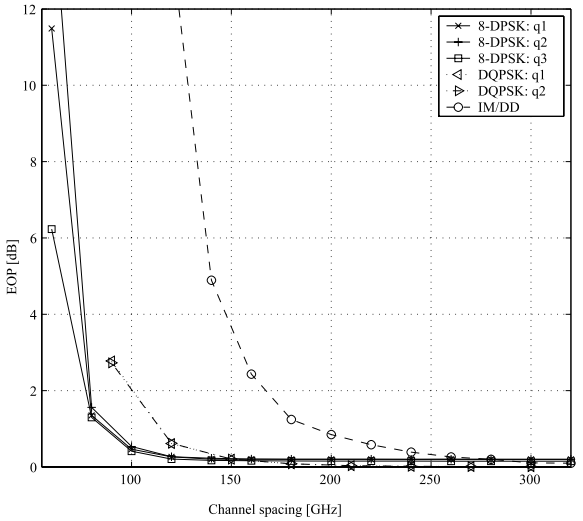

Fig. 5. EOP vs. channel spacing for ch. 5 of an 8-DWDM system with 60 Gbit/s and either 8-DPSK, DQPSK or IM/DD on each channel

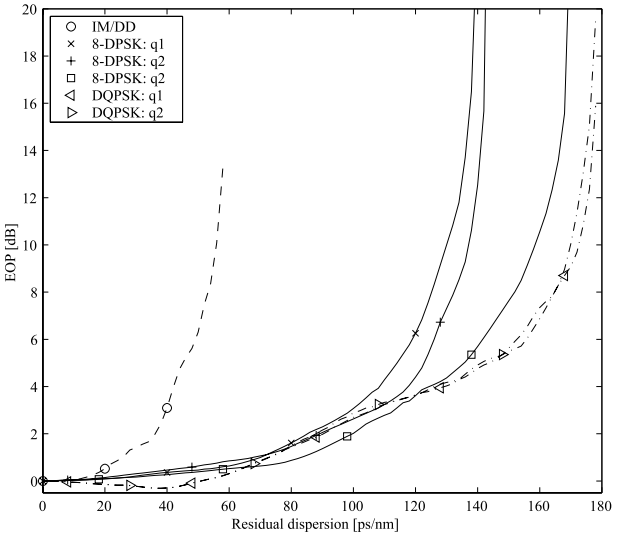

Fig. 6. EOP vs. residual dispersion for 60 Gbit/s single channel transmission using either IM/DD, DQPSK or 8-DPSK

As a consequence, channel spacing in DWDM can be reduced, allowing for higher total bit rates. Eye opening penalties (EOP) from linear crosstalk vs. channel spacing are investigated in Fig. 5. There are three eyes for 8-DPSK (q_1, q_2, q_3) and two eyes for DQPSK (q_1, q_2). Penalties were computed for channel 5 of an 8-DWDM system with 60 Gbit/s per channel. For an EOP of 0.2 dB, the 8-DPSK system allows for a reduction in the channel spacing of more than factor 2.5 compared to IM/DD and about factor 1.5 compared to DQPSK.

In Fig. 6 tolerance to chromatic dispersion is investigated. Again, the total bit rate is 60 Gbit/s, but now single channel systems are used. As expected, 8-DPSK and DQPSK are much more robust against residual dispersion than IM/DD because of the reduced bandwidth. For values of up to around 100 ps/nm 8-DPSK and DQPSK perform similarly. However, if an EOP larger than 3 dB can be tolerated, DQPSK allows for higher residual dispersion. This is surprising, because the 8-DPSK bandwidth is lower than the DQPSK bandwidth. The reason probably lies in the nonlinear signal processing used in the proposed 8-DPSK receiver.

As the 8-DPSK signal has constant mean power, the robustness towards fiber nonlinearties is expected to be higher than for IM/DD as it is the case for DPSK [1] and DQPSK [3]. Detailed studies are in progress for 8-DPSK.

VI. Conclusions

We have presented a transmitter with a differential encoder and a receiver with direct detection for an optical 8-DPSK modulation scheme. The spectral properties are superior to those of previously proposed modulation schemes. This has been shown by a comparison to DQPSK and IM/DD. Because of the high spectral efficiency, 8-DPSK can be used to increase the total bit rate of DWDM systems with a given bandwidth.

References

[1] M. Rohde, C. Caspar, N. Heimes, M. Konitzer, E.-J. Bachus, N. Hanik, "Robustness of DPSK direct detection transmission format in standard fibre WDM systems," Electron. Lett., vol. 35, no. 17, pp. 1483-1484, Aug. 2000.

[2] M. Ohm, J. Speidel, "Quaternary optical ASK-PSK modulation format with direct detection (ASK-PSK/DD)," IEEE Photonics Tech. Lett., vol. 15, no. 1, pp. 159-161, Jan. 2003.

[3] R.A. Griffin, A.C. Carter, "Optical differential quadrature phase-shift key (oDQPSK) for high capacity optical transmission," OFC 2002, Anaheim, paper WX6.

[4] J.G. Proakis, *Digital Communications, Fourth Edition.* New York: McGraw-Hill, 2001.